

Valence Band Electronic Structure of Nb₂Pd_{1.2}Se₅ and Nb₂Pd_{0.95}S₅ Superconductors

H. Lohani^{a,b}, P. Mishra^a, R. Goyal^c, V. P. S. Awana^c, B. R. Sekhar^{a,b,1,*}

^aInstitute of Physics, Sachivalaya Marg, Bhubaneswar 751005, India.

^bHomi Bhabha National Institute, Training School Complex, Anushakti Nagar, Mumbai 400085, India

^cNational Physical Laboratory(CSIR), Dr. K. S. Krishnan Road, New Delhi 110012, India.

Abstract

We present a comparative study of our valence band photoemission results on Nb₂Pd_{1.2}Se₅ and Nb₂Pd_{0.95}S₅ superconductors which is supported by our DFT based electronic structure calculations. We observe that the VB spectra of both the compounds are qualitatively similar, except slight difference in the binding energy position of all features between the two compounds which could be the result of different electronegativity of Se and S atom. The calculated density of states(DOS) reveal that the VB features are mainly composed of Pd-Se/S hybridized states. The nature of DOS originating from the distinctly coordinated Pd atoms is different. Further, the involvement of the various Pd-4d and Nb-4d states in crossing of Fermi level(E_f) signifies the multiband character of these compounds. In addition, we find a temperature dependent pseudogap in Nb₂Pd_{0.95}S₅ which is absent in Nb₂Pd_{1.2}Se₅.

Keywords: , UV Photoelectron spectroscopy, Ternary superconductors, Electronic structure calculation

PACS: 74.25.Jb, 74.70.Dd, 71.20.Be

1. Introduction

Superconducting state of the matter remains as an exciting as well as extensively studied topic from the past. Recently discovered superconductors (SC), like Fe-pnictides[1], Fe-chalcogenides[2], MgB₂[3], SrRuO₄[4], organic SC[5, 6] have added new concepts, like multiband effects, admixture of spin singlet and triplet pairing, spin orbit coupling(SOC) effects *etc.* to the understanding of the superconducting phenomena. Among them Pd based ternary chalcogenides, like Nb₂Pd_{0.95}S₅[7, 8], Nb₂PdSe₅[9], Ta₂PdS₅[10], Ta₂Pd_{0.97}S₆[11], Ta₂Pd_{0.97}Te₆[12] and Ta₄Pd₃Te₁₆[13] show some peculiar behaviors arising from their low dimensional structure and strong SOC.

Nb₂Pd_{1.2}Se₅ and Nb₂Pd_{0.95}S₅ are isomorphic and have their superconducting critical temperature, $T_c \sim 6$ K[7, 9]. Although, Nb₂Pd_{0.95}S₅ shows a Fermi liquid behavior at low temperatures, the value of Sommerfeld coefficient estimated for Nb₂Pd_{1.2}Se₅ and Nb₂Pd_{0.95}S₅, 15.7 and 32 mJ/mol-K² respectively, indicate a moderately and strongly coupled electronic interaction respectively in them. Heat capacity measurements have shown signatures of multiband superconducting behavior in both the compounds which has been well described by the two band- α model. The calculated Fermi surface(FS) of both the compounds exhibit sheets of electron and hole character of different dimensions. Nesting between these 1-D like sheets of FS thought to give rise various density wave orderings, like charge density wave (CDW) and spin density wave (SDW) in these systems[23, 8]. These interesting behaviour could be originated from their complex atomic packing as hybridization strength among different atomic orbitals mainly depends on structural geometry.

Theoretical investigations of the electronic structure of some of these superconducting transition metal chalcogenides, like Nb₂PdSe₅[9], Nb₂PdS₅[8], Ta₂PdS₅[17], Ta₄Pd₃Te₁₆[23] confirm the multiband nature of these compounds. However, till date no direct experimental studies like photoemission has been reported on the valence band

*Corresponding author

Email address: sekhar@iopb.res.in (B. R. Sekhar)

¹Institute of Physics, Sachivalaya Marg, Bhubaneswar-751 005, India
Phone: 91-674-2306412 (Office), Fax: 91-674-2300142

(VB) electronic structure of these class of SCs. In this paper, we present a comparative study of our angle integrated ultra violet photoemission results supported by our DFT based calculations on $\text{Nb}_2\text{Pd}_{1.2}\text{Se}_5$ and $\text{Nb}_2\text{Pd}_{0.95}\text{S}_5$. Our measurements show the VB spectra of both the compounds are qualitatively similar with slight difference in binding energy position of all the features between the two compounds which could be originated due to different electronegativity of Se and S atom. The calculated density of states(DOS) describe the VB features are mainly composed of Pd-Se/S hybridized states. The different nature of DOS originating from the differently coordinated atoms signifies an important role of the complex structural geometry and multiband effects in the electronic structure of these compounds.

2. Experimental and calculation details

Polycrystalline samples of $\text{Nb}_2\text{Pd}_{1.2}\text{Se}_5$ and $\text{Nb}_2\text{Pd}_{0.95}\text{S}_5$ were synthesized via solid state reaction route. Structural and physical properties were studied and reported earlier[7, 9]. Photoelectron spectroscopic studies were performed in angle integrated mode using a hemispherical SCIENTA-R3000 analyzer and a monochromatized He source (SCIENTA-VUV5040). The photon flux was of the order of 10^{16} photons/s/steradian with a beam spot of 2 mm in diameter. Fermi energy (E_f) for all the spectra were calibrated by measuring the E_f of a freshly evaporated Ag film onto the sample holder. The total energy resolution, estimated from the width of the Fermi edge, was about 27 meV for the He I excitation. All the photoemission measurements were performed inside the analysis chamber under a base vacuum of $\sim 3.0 \times 10^{-10}$ mbar. The polycrystalline samples were repeatedly scraped using a diamond file inside the preparation chamber with a base vacuum of $\sim 5.0 \times 10^{-10}$ mbar and the spectra were taken within 1 hour, so as to avoid any surface degradation. All measurements were repeated many times to ensure the reproducibility of the spectra. For the temperature dependent measurements, the samples were cooled by pumping liquid nitrogen through the sample manipulator fitted with a cryostat. Sample temperatures were measured using a silicon diode sensor touching the bottom of the stainless steel sample plate. The low temperature photoemission measurements at 77 K were performed immediately after the cleaning the sample surfaces followed by the room temperature measurements.

First-principles calculations were performed by using plain wave basis set inherent in Quantum Espresso (QE)[24]. Many electron exchange-correlation energy approximated by Perdew-Burke-Ernzerhof (PBE) functional [25, 26, 27] in a scalar relativistic, ultrasoft pseudopotential was employed[28]. Fine mesh of k-points with Gaussian smearing of the order of 0.0001 Ry was used for sampling the Brillouin zone integration. Kinetic energy and charge density cut-off were set to 180 Ry and 900 Ry respectively. Experimental lattice parameters and atomic coordinates of $\text{Nb}_2\text{Pd}_{1.2}\text{Se}_5$ [9] and $\text{Nb}_2\text{Pd}_{0.95}\text{S}_5$ [7] after relaxation under damped (Beeman) dynamics with respect to both ionic coordinates and the lattice vector, were used in the calculations.

3. Results and discussion

Fig.1 shows crystal structure of $\text{Nb}_2\text{Pd}(\text{Se}/\text{S})_5$ which crystallizes in centrosymmetric structure with space group symmetry $C_{2/m}$ (# 12). The lattice parameters of $\text{Nb}_2\text{Pd}(\text{Se}/\text{S})_5$ are $a = 12.788/12.134 \text{ \AA}$, $b = 3.406/3.277 \text{ \AA}$, $c = 15.567/15.023 \text{ \AA}$ and $\beta = 101.63^\circ/103.23^\circ$. The further details of crystal structures regarding Wyckoff positions, site symmetry and fractional occupancies can be obtained from Ref.[9]/[7] for $\text{Nb}_2\text{Pd}(\text{Se}/\text{S})_5$. Both the structures mainly comprise of chains of Pd and Nb polyhedra with Se/S atoms. Pd and Nb atoms are placed at two inequivalent sites with different coordination environment denoted by Pd1, Pd2 and Nb1, Nb2. The atoms denoted by Pd1 are arranged in columns facing their square planarly atoms and in octahedral coordination, whereas, the Pd2 site has a distorted rhombohedral prismatic environment[29]. The Nb atoms form edge sharing and face sharing columns at Nb1 and Nb2 sites respectively and exist in a trigonal prismatic coordination. In packing these Pd and Nb centered polyhedra several octahedral and tetrahedral vacant sites are created. These vacancies lead to site dependent variations in the interorbital hybridization of transition metal atoms with their nearest neighbour (nn) chalcogen atoms due to their different coordination and bond lengths which consequently reflect on the electronic structure of both the compounds.

Fig.2(a) shows valence band (VB) spectra of $\text{Nb}_2\text{Pd}_{1.2}\text{Se}_5$ and $\text{Nb}_2\text{Pd}_{0.95}\text{S}_5$ taken at HeI (21.2 eV) photon energy. In $\text{Nb}_2\text{Pd}_{1.2}\text{Se}_5$, seven features are observed at binding energy (BE) $E_b = -0.27, -1.25, -1.99, -2.53, -3.27, -4.03$ and -5.08 eV which are marked by A to G respectively. The features D, F and G are more intense compared to E and C while the near E_f feature A appears as a hump type structure. The VB spectra of $\text{Nb}_2\text{Pd}_{0.95}\text{S}_5$ is similar

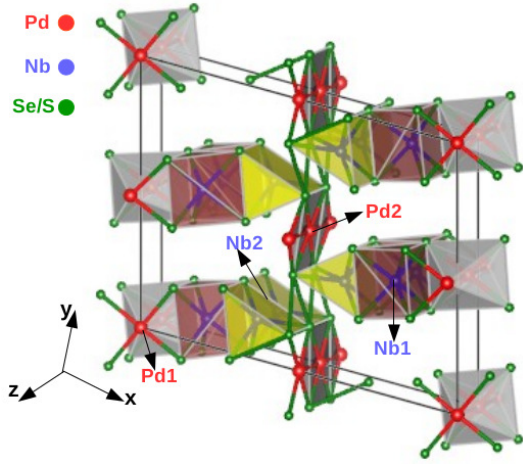


Figure 1: (a) Crystal structure of $\text{Nb}_2\text{Pd}(\text{Se/S})_5$, Pd and Nb atoms at two inequivalent sites are marked.

to that of $\text{Nb}_2\text{Pd}_{1.2}\text{Se}_5$, except that all the features occur at slightly higher BE probably due to its higher resistivity which could be originating from the large electronegativity of S anion in comparison to Se anion. In Fig.2(b) the VB spectra of the two compounds taken at He II (40.8 eV) excitation energy is presented. The He II spectra show sharp enhancement for features A, D and E due to change in the photoemission matrix elements with variation in photon energy. Atomic photoionization cross section (σ) of Pd-4d relative to Se-4p (S-3p) is ~ 8 (14) and 146 (134) for He I and He II respectively[30]. This indicates that features A, D and E are mainly dominated by Pd-4d states in both these compounds. In the cases of both He I and He II, the near E_f spectral weight is lesser in $\text{Nb}_2\text{Pd}_{0.95}\text{S}_5$ compared to $\text{Nb}_2\text{Pd}_{1.2}\text{Se}_5$. This result is again consistent with their conductivity nature which is smaller in case of $\text{Nb}_2\text{Pd}_{0.95}\text{S}_5$ [7] in comparison to $\text{Nb}_2\text{Pd}_{1.2}\text{Se}_5$ [9].

First principles based calculations have been performed on systems with comparable compositions (Nb_2PdSe_5 , and Nb_2PdS_5) in order to have a guidance in interpreting the experimental results. Fig.3(a) and (b) show calculated DOS along with different atomic contributions of Nb_2PdSe_5 and Nb_2PdS_5 respectively. The strongly hybridized states of Pd-4d with their nn Se(S)-p are dominant in VB part \sim BE range $E_b = -7.0$ to -1.0 eV, whereas sufficient states originating from Nb-4d and Se(S)-p hybridization are present in the near E_f region of DOS. These Nb-4d and Se(S)-p hybridized states are also major component in conduction band (CB) region of the DOS in Nb_2PdSe_5 (Nb_2PdS_5). The lower BE of calculated peaks in Nb_2PdSe_5 , in comparison to those of Nb_2PdS_5 , are in agreement with the trends observed in the experimental data of the VB spectra. Similarly, the DOS of both the compounds consist various peak type structures which are not well resolved in the experimental VB spectra. Possible reason for this could be inelastic scattering of the photoelectrons. However, the calculated peaks, which are close to the experimentally observed VB features are labeled with same notation as used in the experimental VB spectra (Fig.2). These results describe the features E, and D mainly derived from Pd-4d states which is consistent with the significant enhancement of these features due to variation in σ of Pd-4d in He II spectra.

As clear from the above results of DOS that the Pd-4d, and Nb-4d states are strongly hybridized with Se/S states. The hybridization could be differ at two distinct coordination sites Pd1 and Pd2 due to different structural environment. In order to provide more insights into the effects of distinct coordination environment m-DOS of Pd is presented in Fig.4. Fig.4 (a) and (b) show Pd-4d states along with different d orbital contributions at Pd1 and Pd2 sites respectively in Nb_2PdSe_5 . Fig.4 (c) and (d) show the same states in Nb_2PdS_5 . The large band width of the Pd-4d seen in both the compounds indicates significant hybridization between the Pd-4d and the nn anion orbitals. In Nb_2PdSe_5 , at the Pd1 site, the $4d_{x^2-y^2}$ and $4d_{xy}$ orbitals are directed towards the square planarly coordinated nn Se atoms and show largest separation between bonding (-4.81 eV and -4.28 eV) and antibonding (1.51 eV) states. The $4d_{3z^2-r^2}$ and $4d_{zx}$ orbitals are oriented towards the nn Pd and Nb atoms and show comparatively smaller separation between bonding (-3.81 eV) and antibonding (0.27 eV) states. This indicates a weak hybridization possibly due to the larger inter-atomic distances Pd1-Pd1 (3.406\AA) and Pd1-Nb1 (3.102\AA) in comparison to the Pd1-Se (2.392\AA). On the other hand,

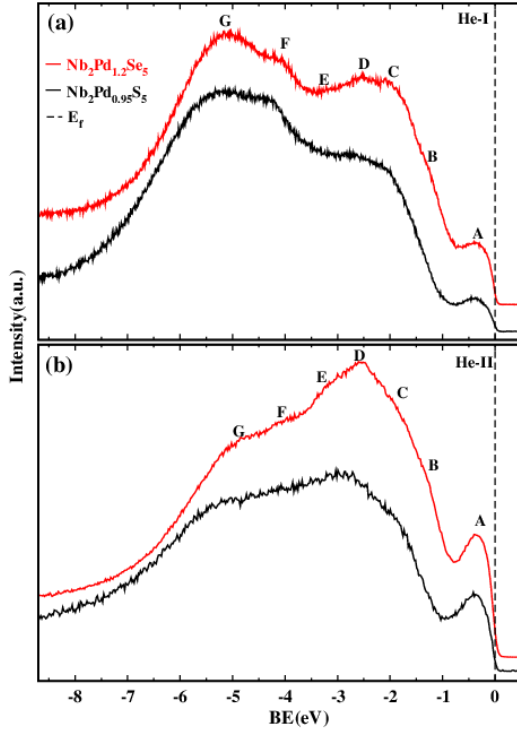


Figure 2: (a) and (b) valence band spectra of $\text{Nb}_2\text{Pd}_{1.2}\text{Se}_5$ (Red) and $\text{Nb}_2\text{Pd}_{0.95}\text{S}_5$ (Black) obtained by using HeI and HeII excitation energy at 300 K respectively.

at the Pd2 site, square planar coordination of the nn Se atoms are aligned in the YZ plane (Fig.1). Therefore, the $4d_{yz}$ orbital is strongly hybridized with the nn Se and antibonding states of this orbital are predominant near the E_f . States originate from $4d_{3z^2-r^2}$, $4d_{xy}$ and $4d_{x^2-y^2}$ orbitals are moderately hybridized while the $4d_{zx}$ states show atomic like character. Apart from the differences in DOS of individual 4d orbitals originating from distinctly coordinated Pd atoms (Pd1, and Pd2), the largest peak of Pd1-4d DOS lies at higher BE relative to same peaks in Pd2-4d DOS. These differences could be related to different interorbital hybridization strengths due to the smaller distance of nn Se atoms at the Pd1 site (2.392 Å) as compared to the Pd2 site (2.598 Å). In case of Nb_2PdS_5 , the orbital character of different 4d orbitals of Pd at both the sites are similar to those of Nb_2PdSe_5 . However, the DOS structure of various 4d orbitals for both Pd1 and Pd2 atoms are slightly different from Nb_2PdSe_5 . This difference could be associated to change in the hybridization strength due to variation in the bond lengths between the two compounds. These results are compared with experimental findings which informs that the higher BE VB features G, and F (Fig.2) fall in bonding states of Pd1 ($4d_{x^2-y^2}$ and $4d_{xy}$) while the $4d_{3z^2-r^2}$ (-1.65 eV) and $4d_{x^2-y^2}$ (-1.35 eV) states of Pd2 are close to the experimentally observed features C and B respectively (Fig.2) in $\text{Nb}_2\text{Pd}_{1.2}\text{Se}_5$. Likewise, the energy position of differently coordinated Pd1 ($4d_{x^2-y^2}$ and $4d_{xy}$) and Pd2 ($4d_{xy}$) states at BE -5.12 eV and -2.09 eV matches closely with the experimental features G and D respectively in the VB spectra of $\text{Nb}_2\text{Pd}_{0.95}\text{S}_5$ (Fig.2). Thus, the qualitative similarity of the experimental data with the calculated DOS could establish the presence of differently coordinated Pd atoms in both the compounds which has also been predicted theoretically in previous reports [8, 17, 9].

In both the compounds Nb atoms also possess distinct coordination environment at two inequivalent sites Nb1 and Nb2, like Pd atoms. We investigate the role of coordination geometry in the DOS of Nb atoms. Fig.5 depicts the Nb-4d DOS with different d orbital contributions at Nb1 and Nb2 sites for Nb_2PdSe_5 (Fig.5(a) and (b)) and Nb_2PdS_5 (Fig.5 (c) and (d)). In both the cases, the DOS of Nb1 and Nb2 is not appreciably differed, unlike the case of Pd DOS. This could be the result of nearly same inter-atomic distances of the Nb atoms with their nn Se/S atoms at both the coordination sites (Nb1 and Nb2). However, a slight difference is visible between the DOS structure of Nb1 and Nb2 in the vicinity of E_f which could be an important factor in the electronic structure of these compounds. Further, the

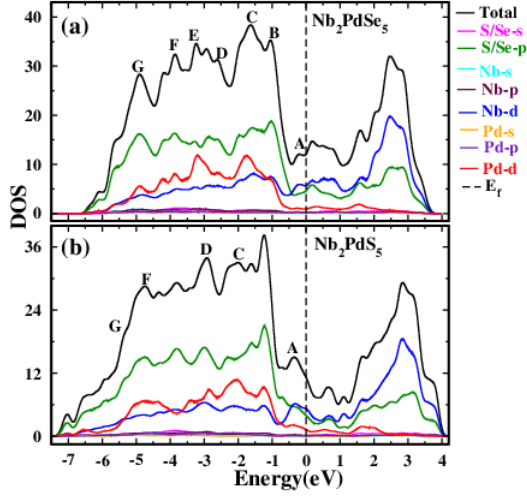


Figure 3: (a) and (b) calculated Total DOS with different atomic contributions of Nb_2PdSe_5 and Nb_2PdS_5 respectively.

orbital character of states which are predominantly involved in the E_f crossing is $4d_{3z^2-r^2}$, and $4d_{zx}$ orbitals of Nb1 and $4d_{xy}$ of Nb2. This result, as well as similar behaviour of the E_f crossing by orbital specific Pd-4d DOS (see Fig.4) are signature of multiband nature of these compounds which is consistent with the observed multigap behavior in heat capacity measurements on these compounds [7, 9]. These calculated results are also in good agreement with previous reports [17, 8, 9].

Fig.6(a) and (b) show a comparison between the VB spectra of $\text{Nb}_2\text{Pd}_{1.2}\text{Se}_5$ and $\text{Nb}_2\text{Pd}_{0.95}\text{S}_5$ at 300 K and 77 K using He I and He II excitation energy, where differences between the normalized spectra collected at 300 K and 77 K are also plotted in each graph in order to highlight the temperature dependent changes. In case of $\text{Nb}_2\text{Pd}_{1.2}\text{Se}_5$, the near E_f states remain unchanged with the lowering of temperature. On the other hand, $\text{Nb}_2\text{Pd}_{0.95}\text{S}_5$ spectra shows a depletion of spectral weight near the E_f which is more pronounced in case of He II. This suppression of DOS is a signature of a pseudogap. In addition, an earlier study shows a crossover of transport carriers from electron to hole has been found at 100 K in Hall measurements in this compound [7]. These two observations are consistent with previous report describing a pseudogap driven sign reversal in Hall coefficients [32]. On the other hand, in $\text{Nb}_2\text{Pd}_{1.2}\text{Se}_5$ the energy scale $T \sim 50$ K, below which a crossover in the electronic ground state has been realized in the transport measurements [9] is lower than our measurement temperature 77 K. This could possibly be the reason for the unseen pseudogap feature at 77 K in $\text{Nb}_2\text{Pd}_{1.2}\text{Se}_5$.

4. Conclusion

We have presented a comparative study of the VB electronic structure of $\text{Nb}_2\text{Pd}_{1.2}\text{Se}_5$ and $\text{Nb}_2\text{Pd}_{0.95}\text{S}_5$ in conjunction with DFT based calculations. We find the VB spectra of both the compounds are qualitatively similar, though all the features are observed at slightly higher BE in $\text{Nb}_2\text{Pd}_{0.95}\text{S}_5$ relative to $\text{Nb}_2\text{Pd}_{1.2}\text{Se}_5$ which could be the result of larger electronegativity of S anion in comparison to Se anion. The calculated DOS describe the VB features are mainly composed of Pd-Se/S hybridized states. The different nature of DOS originating from the differently coordinated atoms signifies an important role of the complex structural geometry in the electronic structure of these compounds. In addition, in our calculated DOS, states crossing the E_f are dominated by different Pd-4d and Nb-4d orbitals ensuring significant role of multiband effects in these compounds. Furthermore, $\text{Nb}_2\text{Pd}_{0.95}\text{S}_5$ spectra exhibits a depletion of spectral weight near the E_f with lowering the temperature to 77 K which results a pseudogap feature. This observation is consistent with previous finding of sign reversal in Hall coefficients below the temperature 100 K. On the other hand, temperature dependent pseudogap is absent in case of $\text{Nb}_2\text{Pd}_{1.2}\text{Se}_5$ which could be due to the energy scale $T \sim 50$ K of crossover in the electronic ground state is lower than our measurement temperature 77 K. Our comprehensive valence band electronic structure study in these compounds may open ways for further experimental and theoretical investigations in this field.

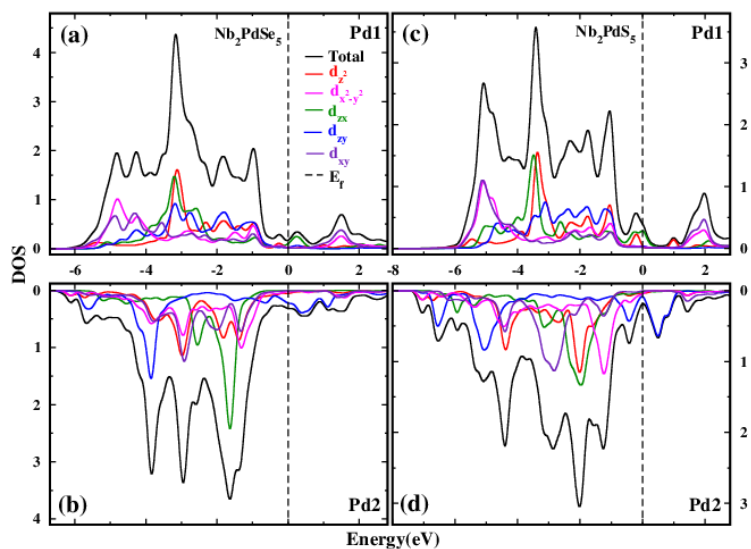


Figure 4: (a) and (b) DOS originated from different orbitals of Pd-4d at sites Pd1 and Pd2 respectively in Nb_2PdSe_5 . (c) and (d) show the same DOS at Pd1 and Pd2 site respectively in Nb_2PdS_5 .

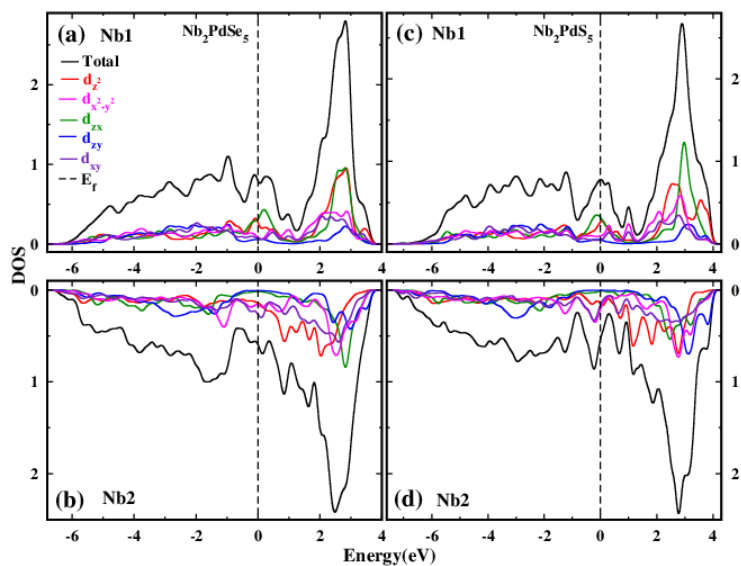


Figure 5: DOS originated from different orbitals of Nb-4d at site Nb1 and Nb2 are shown in (a) and (b) respectively in Nb_2PdSe_5 . (c) and (d) show same DOS at Nb1 and Nb2 site respectively in Nb_2PdS_5 .

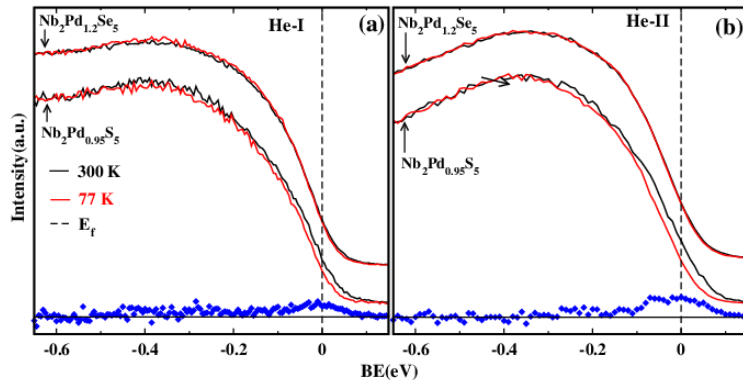


Figure 6: Comparison between 300K (Black) and 77K (Red) near E_f VB spectra, of $\text{Nb}_2\text{Pd}_{1.2}\text{Se}_5$ and $\text{Nb}_2\text{Pd}_{0.95}\text{S}_5$ taken at (a) HeI and (b) HeII source energy. Blue dotted points represent the difference between spectra collected at 300K and 77K of $\text{Nb}_2\text{Pd}_{0.95}\text{S}_5$.

References

- [1] G. R. Stewart *Rev. Mod. Phys.* **83** (2011) 1589.
- [2] Y. Mizuguchi and Y. Takano *J. Phys. Soc. Jpn.* **79** (2010) 102001.
- [3] A. Gurevich, S. Patnaik, V. Braccini, K. H. Kim, C. Mielke, X. Song, L. D. Cooley, S. D. Bu, D. M. Kim, J. H. Choi, L. J. Belenky, J. Giencke, M. K. Lee, W. Tain, X. Q. Pan, A. Siri, E. E. Hellstrom, C. B. Eom and D. C. Larbalestier *Supercond. Sci. Technol.* **17** (2004) 278.
- [4] A. P. Mackenzie, Y. Maeno *Rev. Mod. Phys.* **75** (2000) 657.
- [5] M. R. Norman *Science* **332** (2011) 196.
- [6] K. Bechgaard, K. Carneiro, M. Olsen, F. B. Rasmussen, C. S. Jacobsen *Phys. Rev. Lett.* **46** (1981) 852.
- [7] R. Jha, B. Tiwari, P. Rani, H. Kishan and V. P. S. Awana *J. Appl. Phys.* **115** (2014) 213903.
- [8] Q. Zhang, G. Li, D. Rhodes, A. Kiswandhi, T. Besara, B. Zeng, J. Sun, Siegrist, M. D. Johannes and L. Balicas *Scientific Reports* **3** (2013) 1446.
- [9] Seunghyun Khim, Bumsung Lee, Ki-Young Choi, Byung-Gu Jeon, Dong Hyun Jang, Deepak Patil, Seema Patil, Rokyeon Kim, Eun Sang Choi, Seongsu Lee, Jaeyun Yu and Kee Hoon Kim *New J. Phys.* **15** (2013) 123031.
- [10] Y. F. Lu, T. Takayama, A. F. Bangura, Y. Katsura, D. Hashizume and H. Takag *J. Phys. Soc. Japan* **83** (2014) 023702.
- [11] B. Tiwari, B. B. Prasad, R. Jha, D. K. Singh and V. P. S. Awana *J. of Super. Nov. Magn.* **27** (2014) 2181.
- [12] R. Goyal, B. Tiwari, R. Jha, and V. P. S. Awana *J. of Super. Novel. Magn.* **28** (2015) 119.
- [13] Wen-Hu Jiao, Zhang-T Tang, Yun-Lei Sun, Y. Liu, Q. Tao, Chun-Mu Feng, Yue-Wu Zeng, Zhu-An Xu and Guang-Han Cao *J. of Am. Chem. Soc.* **136** (2014) 1284.
- [14] B. S. Chandrasekhar *Appl. Phys. Lett.* **1** (1962) 7.
- [15] A. M. Clogston *Phys. Rev. Lett.* **9** (1962) 266.
- [16] C. Q. Niu, J. H. Yang, Y. K. Li, Bin Chen, N. Zhou, J. Chen, L. L. Jiang, B. Chen, X. X. Yang, Chao Cao, Jianhui Dai, and Xiaofeng Xu *Phys. Rev. B* **88** (2013) 104507.
- [17] David J. Singh *Phys. Rev. B* **88** (2013) 174508.
- [18] N. Zhou, Xiaofeng Xu, J. R. Wang, J. H. Yang, Y. K. Li, Y. Guo, W. Z. Yang, C. Q. Niu, Bin Chen, Chao Cao, Jianhui Dai *Phys. Rev. B* **90** (2014) 094520.
- [19] Masahiro Takahashi, Takeshi Mizushima and Kazushige Machida *Phys. Rev. B* **89** (2014) 064505.
- [20] D. A. Zocco, K. Grube, F. Eilers, T. Wolf and H. v. Lohneysen *Phys. Rev. Lett.* **111** (2013) 057007.
- [21] Suk Joo Youn, Mark H. Fischer, S. H. Rhim, Manfred Sigrist, and Daniel F. Agterberg *Phys. Rev. B* **85** (2012) 220505(R).
- [22] Jun Goryo, Mark H. Fischer and Manfred Sigrist *Phys. Rev. B* **86** (2012) 100507(R).
- [23] David J. Singh *Phys. Rev. B* **90** (2014) 144501.
- [24] Giannozzi P. et al. <http://www.quantum-espresso.org>.
- [25] Perdew J P, Burke K and Ernzerhof M *Phys. Rev. Lett.* **77** (1996) 3865.
- [26] Perdew J P and Wang Y *Phys. Rev. B* **45** (1992) 13244.
- [27] Perdew J P, Chevary J A, Vosko S H, Jackson K A, Pederson M R, Singh D J and Fiolhais C *Phys. Rev. B* **46** (1992) 6671.
- [28] Vanderbilt D Soft self-consistent pseudopotential in a generalized eigenvalue formalism *Phys. Rev. B* **41** (1990) 7892.
- [29] D. A. Keszler, J. A. Ibers, S. Maoyu and L. Jiaxi *J. of Solid State Chem.* **57** (1985) 68.
- [30] J. J. Yeh and I. Lindau *Atomic Data and Nuclear Data Tables* **32** (1985) 1-155.
- [31] P. Larson, V. A. Greanya, W. C. Tonjes, R. Liu, S. D. Mahanti and C. G. Olson *Phys. Rev. B* **65** (2002) 085108.
- [32] D. V. Evtushinsky, A. A. Kordyuk, V. B. Zabolotnyy, D. S. Inosov, B. Buchner, H. Berger, L. Patthey, R. Follath, and V. Borisenko, *Phys. Rev. Lett.* **100** (2008) 236402.
- [33] Alexander Gabovich, A I Voitenko and Toshikazu Ekino *J. Phys. Condens Matter* **16** (2004) 3681.